Epitaxial growth of gallium oxide films on c-cut sapphire substrate

W. Seiler [a], M. Selmane [b,c], K. Abdelouhadi [b,c], J. Perrière [b,c,*]

[a] PIMM, UMR CNRS 8006, Arts et Métiers ParisTech, 151, Boulevard de l'Hôpital, 75013 Paris, France
[b] Sorbonne Universités, UPMC Univ Paris 06, UMR 7588, INSP, F-75005 Paris, France
[c] CNRS, UMR 7588, INSP, F-75005 Paris, France

A B S T R A C T

The nature of the crystalline phase present in gallium oxide films grown by pulsed-laser deposition on c-cut sapphire substrate has been studied. Amorphous, polycrystalline or epitaxial gallium oxide films can be obtained depending upon the oxygen pressure during the growth in the 400–500 °C temperature range. Detailed pole figure measurements on epitaxial films demonstrate that the monoclinic β-Ga_2O_3 phase grows epitaxially on c-cut sapphire substrates at T = 500 °C under a 10^{-5} mbar oxygen pressure. Two distinct textures were evidenced, i.e., the $(\bar{2}01)$ and (101) planes of the monoclinic β-Ga_2O_3 phase being parallel to the c-cut sapphire substrates. The corresponding epitaxial relationships were determined and interpreted in the frame of the domain matching epitaxy. The differences in the two textures were correlated to the various atomic configurations in the $(\bar{2}01)$ and (101) planes of the monoclinic β-Ga_2O_3 phase.

Keywords:
Gallium oxide
Laser ablation
X-ray diffraction
Epitaxial relationships
Growth models

1. Introduction

Gallium oxide is a wide band gap (4.9 eV) material, whose physical properties can lead to applications in various domains [1–6]. As a result, the growth of Ga_2O_3 thin films has been studied by the main chemical and physical deposition methods [7–14]. The structural characteristics and physical properties of these gallium oxide films are very sensitive to the growth conditions [15], so that the films can be either electrically insulating or conductive, opaque or transparent, and crystalline or amorphous [11,12]. Moreover, the importance of oxygen composition was evidenced [16], through a chemically driven insulator to metal transition in highly deficient gallium oxide ($Ga_2O_{2.44}$) films. These results were explained by the formation of a sub-stoichiometric and conducting phase mixed with a stoichiometric Ga_2O_3 insulating phase [16]. For larger oxygen deficiencies ($Ga_2O_{2.3}$), the oxide was found to be not stable, and a phase separation occurs leading to the synthesis of Ga nanoparticles in a stoichiometric Ga_2O_3 matrix [11,12], i.e., formation of nanocomposite oxide films. Resistivity measurements of such nanocomposite films evidence the melting and the freezing of the Ga clusters, and their superconducting transition [11,12]. Such an influence of the oxygen deficiency on the nature and properties of oxide films has also been evidenced in other oxide compounds [17–20], by the formation of nanocomposite oxide films via the phase separation.

The structural characteristics of these oxygen deficient Ga oxide films have not been precisely presented [11,16]. The aim of this paper is thus to report on the structural characteristics (nature of phase, film textures and epitaxial relationships with the substrate) of Ga oxide films formed on c-cut sapphire substrates. Bulk Ga_2O_3 has been reported to crystallize in five different structures, i.e., the α, β, δ, γ and ε phases, but the β-Ga_2O_3 monoclinic phase (a = 1.223 nm, b = 0.304 nm, c = 0.580 nm and β = 103.70°) is the most stable whereas the all other polymorphs are not stable and transform into the β phase at sufficiently high temperature. In the case of thin film on c-cut sapphire substrates, the β monoclinic phase has been generally observed [7,9,10,14], but the presence of the hexagonal α phase has been also reported [21]. Some works have shown that the crystalline structure of doped or not Ga oxide films could not be identified with the β monoclinic phase [22–24]. Indeed the X-ray diffraction diagrams could be due to the not clearly known ε phase [22]. Moreover, it was suggested that this ε phase could be described with an orthorhombic structure [24]. The precise axes parameters and stability domain of this possible orthorhombic (a = 0.512 nm, b = 0.879 nm, c = 0.941 nm) ε phase were further studied and calculated [25]. In this paper we present results dealing with the nature (monoclinic or orthorhombic) of the crystalline phases present in Ga oxide films formed by pulsed-laser deposition (PLD), on c-cut sapphire substrates. Depending upon the conditions, amorphous polycrystalline or epitaxial films have

* Corresponding author at: Sorbonne Universités, UPMC Univ Paris 06, UMR 7588, INSP, F-75005 Paris, France.
E-mail address: Jacques.Perriere@insp.jussieu.fr (J. Perrière).

been obtained. This paper emphasizes the case of epitaxial growth of the monoclinic β-Ga_2O_3 phase, whose precise texture and in plane epitaxial relationships with the substrate have been determined and described in the frame of the domain matching epitaxy [26,27].

2. Experimental

Ga oxide thin films (in the 50 to 500 nm thickness range) were grown by PLD by focusing a frequency quadrupled Nd:YAG laser ($\lambda = 266$ nm, $\tau = 7$ ns, 5 Hz repetition rate) onto a Ga_2O_3 ceramic target, the experimental set-up being presented elsewhere [28]. Pulses in the 0.5 to 2 J/cm^2, i.e., in the 50 to 200 · 10^6 W/cm^2 power density range, were fired on the target, whose distance to the substrate was equal to 5.5 cm. The film growth on c-cut sapphire substrates was carried out under controlled pressure, between the base pressure ($5 \cdot 10^{-7}$ mbar) up to 0.1 mbar in oxygen pressure. The substrate temperature was regulated in the 300 to 500 °C range. After the deposition, films were allowed to cool to room temperature under the same oxygen pressure used for the growth.

The thickness and composition of the films were determined by Rutherford backscattering spectrometry (RBS), using the 2 MeV Van de Graaff accelerator of the INSP. Such measurements gave composition determination for the Ga cations, with a rather good accuracy, while the oxygen content was only determined with a 4% precision, owing to the low RBS yield on light elements like oxygen.

The crystalline structure of the films was studied by X-ray diffraction analyses (XRD) using the PANalytical Xpert MRD diffractometer at the INSP and at the ENSAM. The nature of the phases was investigated either in the Bragg–Brentano mode or in the grazing incidence geometry, and by asymmetric diffraction, i.e., pole figure measurements [9,29]. In this last geometry, the epitaxial relationships between gallium oxide films and single crystal substrates were studied and the precise in-plane orientations between film and substrate were determined.

3. Results and interpretations

Previous studies on the PLD process have shown that the oxygen incorporation in oxide films can be controlled by the laser fluence and oxygen pressure P_{O_2} during the growth [17,30–32]. It follows that the pertinent parameter governing the nature, composition and properties of the Ga oxide films is the ratio of the flux of gallium [Ga] and oxygen [O] atoms reaching the surface of the growing film, i.e., the ratio [Ga]/[O] [31].

For high P_{O_2} (10^{-1} mbar), the oxygen flux is largely higher than the Ga flux emitted by the target, and stoichiometric Ga_2O_3 films are grown [11,12]. For decreasing oxygen pressure (down to 10^{-4} mbar), the ratio [Ga]/[O] increases and as a result, the incorporation of oxygen atoms in the films decreases, leading to the formation of oxygen deficient Ga oxide, i.e., Ga_2O_x with $2.5 < x < 3$. On the other hand, the films grown under vacuum ($5 \cdot 10^{-7}$ mbar), are largely oxygen deficient (Ga_2O_x with $x < 2.3$). Between these two extreme cases, an intermediate situation can be observed. Indeed, at 10^{-5} mbar and moderate laser power density, insulating and slightly absorbing $Ga_2O_{2.5}$ films are grown.

In the present work, all the Ga oxide films grown on c-cut sapphire substrates at P_{O_2} higher than 10^{-5} mbar and $T < 400$ °C were found to be optically transparent, insulating and amorphous [11,12]. Such a behavior has been already reported [23], and it could be the consequence of the disorder introduced by the significant oxygen deficiency and/or to the low substrate temperature, which does not allow the crystallization of the films.

The films grown under vacuum (residual pressure: $5 \cdot 10^{-7}$ mbar) were found to be widely oxygen deficient ($Ga_2O_{2.3}$), optically absorbing in the UV–Visible domain, electrically conducting [11] and polycrystalline. Fig. 1 represents typical diffraction patterns (in the grazing incidence geometry) for a film corresponding to a $Ga_2O_{2.3}$ composition. Numerous broad and low intensity peaks superimposed on a noticeable

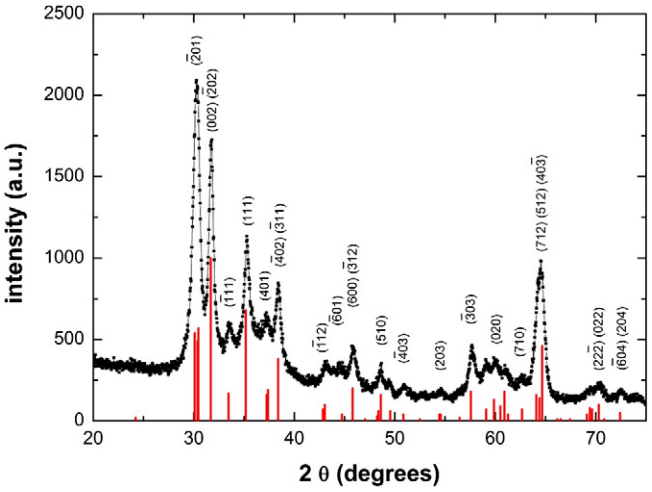

Fig. 1. X-ray diffraction diagram in grazing incidence for a gallium oxide films grown on a c-cut sapphire substrate at 400 °C under $5 \cdot 10^{-7}$ mbar (residual pressure).

background are observed in this diagram, indicating that a fraction of the film is in the amorphous state. For comparison purpose, the position and intensity of the diffraction peaks of the monoclinic β-Ga_2O_3 phase (as given in the JCPDS 43-1012 file) are presented in this figure. A rather good agreement is observed between the peak positions and the experimental diagram which would indicate that the β-Ga_2O_3 phase is formed in the film grown under residual pressure. Previously [22] it has been reported that the diffraction diagrams of gallium oxide films could be identified with the diffraction peaks of the ε-Ga_2O_3 phase (JCPDS 11-0342 file). As the angular position of some of the diffraction peaks of this ε phase are very close to those of the β-Ga_2O_3 phase, it is not a priori possible to completely exclude the presence of this phase in the film.

In the intermediate oxygen pressure regime (about 10^{-5} mbar), crystalline gallium oxide thin films on sapphire substrates were obtained for temperatures higher than 400 °C. Fig. 2 represents a typical XRD diagram recorded in the Bragg–Brentano geometry, for a film grown at 10^{-5} mbar and 500 °C. Three intense and well defined peaks are observed in this diagram. These three peaks were already reported in the literature for Ga oxide films grown on c-cut sapphire [23,24], and can be attributed to either the $(\bar{2}01)$, $(\bar{4}02)$ and $(\bar{6}03)$ planes of the

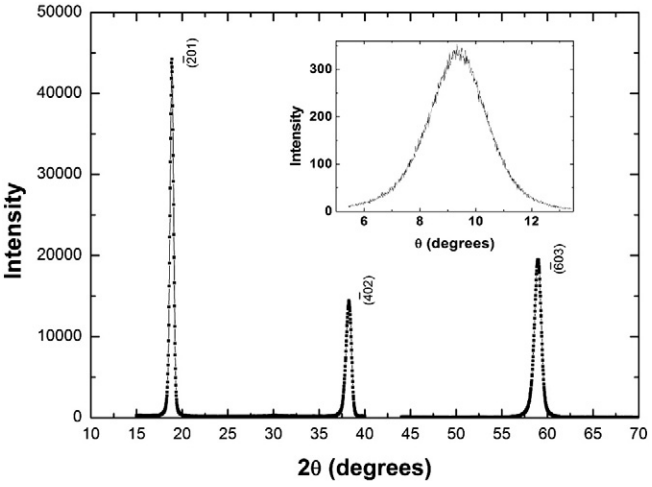

Fig. 2. X-ray diffraction diagram in the Bragg–Brentano geometry for a gallium oxide film grown in a c-cut sapphire substrate at 500 °C under 10^{-5} mbar. The inset shows the rocking curve recorded for the peak at $2\theta = 38.5°$.

monoclinic β-Ga_2O_3 phase, or the (002), (004) and (006) planes of the orthorhombic phase which has been proposed as the crystalline structure of the ε phase [24]. Accordingly, these films present either a ($\bar{2}$01) texture (monoclinic phase) or a (002) texture (orthorhombic phase). The rocking curve corresponding to the 18.9° peak is presented in the inset of Fig. 2 and shows a rather wide FWHM (more than 2°), i.e., the mosaicity of such films is important.

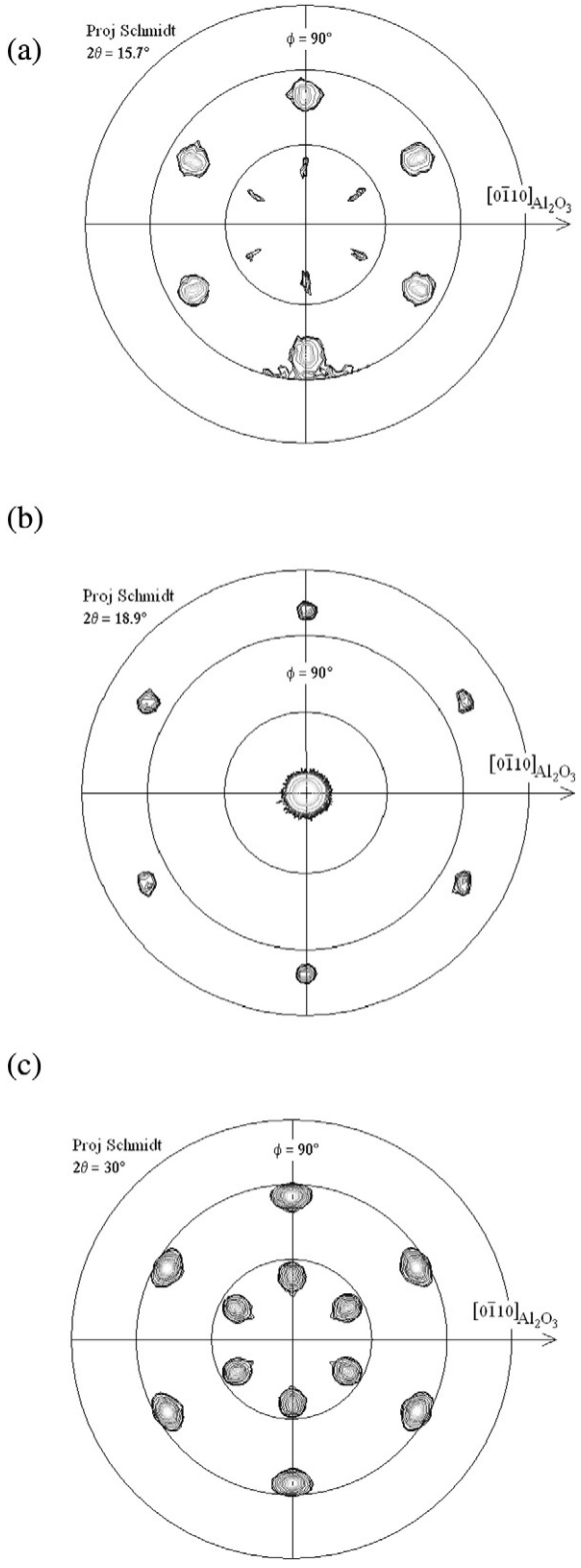

Fig. 3. Pole figures recorded on a gallium oxide film grown in a c-cut sapphire substrate at 500 °C under 10^{-5} mbar for 2θ values equal to 15.7° (a), 18.85° (b) and 31.7° (c).

The simple XRD diagram presented in Fig. 2 does not permit to choose between the two Ga_2O_3 phases, the β monoclinic and the orthorhombic phase previously described [25]. To gain more information on the nature of the phase, asymmetric diffraction was used through pole figure measurements [9,29]. Fig. 3 represents typical poles figures recorded on a film grown at 10^{-5} mbar and 500 °C, with the following 2θ values: 15.7, 18.9 and 30°. The first one (15.7°) is only present in the monoclinic β-Ga_2O_3 phase, while the others correspond to diffracting planes present in both the monoclinic and orthorhombic phases. All these pole figures present intense and well defined poles indicating that epitaxial gallium oxide film has been grown on the c-cut sapphire substrate.

For a given pole figure corresponding to a diffraction angle 2θ, it is possible to calculate the declination angles ψ associated with the diffracting planes in the monoclinic and orthorhombic structure respectively. Then it is possible to compare these theoretical values to those experimentally deduced from the pole figures, and Table 1 presents these results. For each 2θ value, the experimental values of ψ are given, as well as the diffracting planes (hkl) of the monoclinic and orthorhombic phases corresponding to the 2θ value, and the expected declination angle ψ for the two phases. Table 1 shows thus that the poles observed in Fig. 3 cannot be due to the orthorhombic phase. Actually the calculated ψ values of the poles for this orthorhombic phase [25] are generally largely different from those experimentally observed, and only a few ones are in agreement. It is thus possible to exclude the presence of the orthorhombic phase in the film.

On the contrary all the poles in Fig. 3 can be interpreted in the frame of the monoclinic β-Ga_2O_3 phase but with two different textures. In fact by looking at Fig. 3b, obtained for 2θ value equal to 18.9°, i.e., the diffracting angle of the ($\bar{2}$01) plane of the β-Ga_2O_3 phase, one can observe a central pole (corresponding to crystallites with the ($\bar{2}$01) texture), and six poles located at a declination angle ψ = 72.5°. These six poles cannot be due to crystallites with the ($\bar{2}$01) texture, and are solely explained by assuming the presence of crystallites with the (101) texture. Indeed, the calculated ψ value for the (101) oriented crystallites corresponds exactly to the experimental value of the declination angle. In the same way, for 2θ = 15.7° (Fig. 3a), the poles observed at ψ = 50° are due to the ($\bar{2}$01) oriented crystallites, while the poles present at ψ = 23° correspond to (101) oriented crystallites. On all the pole figures, the poles were identified with diffracting planes of crystallites presenting either the ($\bar{2}$01) or (101) textured orientation (see Table 1).

Let us notice that a diffraction peak corresponding to the (101) plane of the β-Ga_2O_3 phase is not observed in the diffraction diagram (Fig. 2), owing to the extinction rules of the monoclinic phase (see JCPDS 43-1012 file). On the other hand, the ($\bar{2}$01) and (101) planes show a very similar rectangular lattice with the following lattice parameters a = 0.304 nm and b = 1.472 nm for the (101) plane and a = 0.304 nm and b = 1.469 nm for the ($\bar{2}$01) plane. Moreover, these two families of planes are polar, i.e., planes only constituted by either oxygen or gallium atom, and this point can play a role on the growth mechanism (see below). Despite these similarities, a difference appears between these two textures. Indeed, in Fig. 3b, the sum of the intensity of the 6 poles corresponding to the (101) crystallites is about 7 times lower than that of the single central pole characteristics of the ($\bar{2}$01) texture. The ($\bar{2}$01) texture appears thus most likely than the (101) one, i.e., the ($\bar{2}$01) texture is more energetically favorable for the growth of the β-Ga_2O_3 phase on c-cut sapphire substrates than the (101) texture.

Previously it was reported that epitaxial ($\bar{2}$01)-oriented β-Ga_2O_3 films were grown on c-cut sapphire substrates grown by various methods [7,10,14,33,34]. In these previous papers, pole figure measurements were not presented, the epitaxial growth of the β-Ga_2O_3 phase

Table 1
Experimental and calculated ψ values for the β-monoclinic and orthorhombic Ga_2O_3 phases for some diffraction peaks of the films.

2θ (°)	Ψ (°) exp	Ψ monoclinic β			Ψ orthorhombic	
		(hkl)	Texture $(\bar{2}01)$	Texture (101)	(hkl)	Texture (002)
15.7	23	(001)	49.97	22.5		
	50	(001)				
18.9	0	$(\bar{2}01)$	0	72.50	(002)	0
	72.5					
24	15	(201)		14.46		
30	24	$(\bar{4}01)$	23.47	53.78	(013)	19.64
	54	(400)	53.73			
31.7	23	$(\bar{2}02)$	22.5	22.52	(031)	72.71
	50	(002)	49.97	49.99	(122)	54.67
		$(\bar{2}02)$				
		(002)				
38.3	0	$(\bar{4}02)$	0	72.50	(004)	0
	53	$(\bar{3}11)$	52.9			
	72.5	$(\bar{4}02)$				
48.6	47	$(51\bar{1})$	46.85	62.27	(213)	51.93
	63	(510)	62.23		(231)	78.42
58.3	0	$(\bar{6}03)$	0	72.50	(006)	0
	38.5	$(\bar{3}13)$	38.24		(035)	32.72
	72.5	(603)			(312)	70.41
64	36	$(\bar{2}04)$	36.23	36.26	(205)	36.33
	72	$(22\bar{1})$	72.12	72.13	(135)	36.50
		(121)				

was only deduced from ϕ scan measurements which do not permit to evidence the existence of the (101) texture in the films. More recently, monoclinic β-Ga_2O_3 films have been prepared by Ga evaporation in oxygen plasma on c-cut sapphire substrates [9] and a pure $(\bar{2}01)$ texture was solely observed in X-ray diffraction analysis (Bragg–Brentano mode and pole figure measurements), the (101) texture being not observed. The origin of this difference with the present work has to be related the different growth methods, i.e., Ga evaporation in oxygen plasma [9] and PLD of a Ga_2O_3 target in this work. More precisely, for Ga evaporation in oxygen plasma, the deposition rate was kept in the 0.1 to 0.15 nm/s range at 800 °C [9]. Due to this low deposition rate and to the high substrate temperature (800 °C), the incident species could diffuse on long distances in order to find the lower energy crystallographic site. The formation of the most energetically favorable texture will thus occur in these conditions, i.e., the $(\bar{2}01)$ texture will be observed. On the contrary, in PLD a high deposition rate per pulse (about 0.1 nm per pulse) is observed as it is the case in the pulsed-energy deposition methods [35]. Assuming a 10 μs duration time of arrival of the species emitted by the target during a laser pulse, the instantaneous deposition rate can be estimated of the order of 10^4 μm/s. With such a high instantaneous deposition rate and a lower substrate temperature (500 °C), the high flux of species reaching the surface of the growing film will "quench" at least partly the film structure, as atoms will not have sufficient time to migrate at the film surface to find the most favorable crystallographic site. As a result both the $(\bar{2}01)$ and (101) textures will be observed in films grown by PLD, despite the fact that the $(\bar{2}01)$ texture seems more energetically favorable for the growth of the β-Ga_2O_3 phase on c-cut sapphire substrates than the (101) texture.

In Fig. 3, the $[0\bar{1}10]$ in-plane direction of the c-cut sapphire substrates is indicated in each pole figure, and this allows deducing the in-plane epitaxial relationships between the film and the substrates for the two textures:

$$[102]_f//[10.0]_s \text{ and } [010]_f//[21.0]_s \quad \text{for the } \left(\bar{2}01\right) \text{ texture}$$
$$\left[\bar{1}01\right]_f//[10.0]_s \text{ and } [010]_f//[21.0]_s \quad \text{for the } (101) \text{ texture}$$

where the subscripts f and s stand for the gallium oxide film and c-cut sapphire substrate respectively.

Fig. 4a schematically represents this epitaxial relationships through the superposition of the rectangular $(\bar{2}01)$ β-Ga_2O_3 plane on the hexagonal (0001) sapphire plane. As the $(\bar{2}01)$ and (101) β-Ga_2O_3 planes present a similar rectangular lattice, the case of the $(\bar{2}01)$ plane is solely shown in this figure. The schema presented in Fig. 4a and its variants corresponding to the three-fold symmetry of the (0001) sapphire plane and the two-fold symmetry of the $(\bar{2}01)$ (or (101)) β-Ga_2O_3 plane, explain the poles observed in Fig. 3. In addition to the difference in lattice symmetry, a noticeable lattice mismatch exists, especially along the [010] axis of the film. In such a case, the epitaxial relationships can be classically interpreted in the frame of the domain matching epitaxy or extended atomic distance mismatch approach [26,27], in which m lattice units of the film match with p lattice units of the substrate. The values of m and p are defined as the minimum integers which satisfy the relation:

$$md_f \approx pd_S \text{ or } d_f/d_S \approx p/m$$

d_f and d_s being the respective lattice parameter in the film and substrate parallel directions [26,27]. The corresponding lattice mismatch δ can therefore be defined [27] by:

$$\delta = 2[md_f - pd_S]/[md_f + pd_S].$$

These results are summarized in Table 2. Due to the similarity in lattice for the $(\bar{2}01)$ and (101) planes, very similar values of lattice mismatch are obtained.

It has to be noticed that the poles in Fig. 3 present a broad azimuthal extension. This could be due to a large in-plane mosaicity of the crystallite orientation, but it could also be due to the presence of another in-plane epitaxial orientation as it has been previously observed [36]. Indeed, Fig. 4b shows this other epitaxial relationship, related to the following alignment:

$$[132]_f//\left[1\bar{1}.0\right]_s \quad \text{for the } \left(\bar{2}01\right) \text{ texture}$$
$$[131]_f//\left[1\bar{1}.0\right]_s \quad \text{for the } (101) \text{ texture.}$$

The corresponding matching and lattice mismatch are given in Table 2, and are very similar. The epitaxial relationships schematized

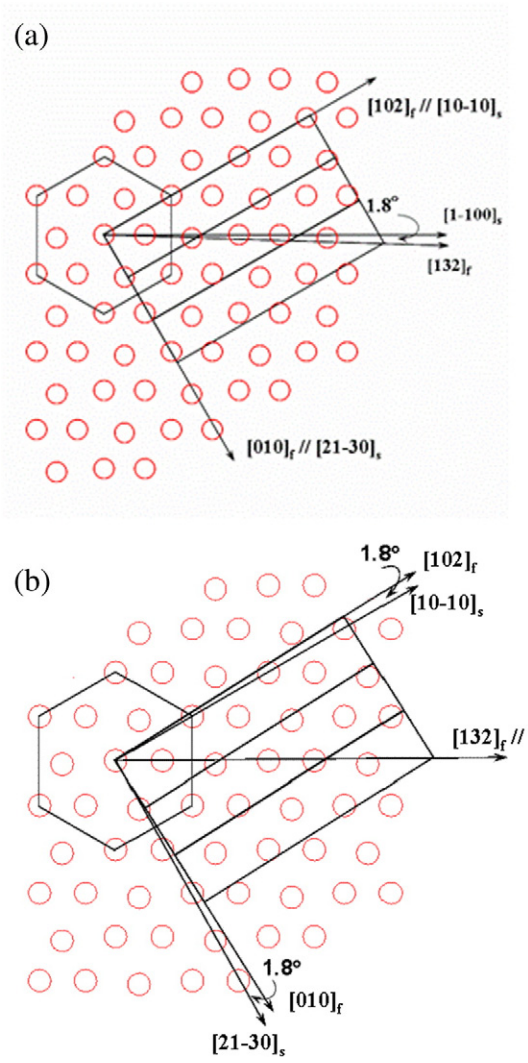

Fig. 4. Schematic representation of the first (a) and second (b) possible in-plane epitaxial relationships between the $(\bar{2}01)$ oriented gallium oxide film and the c-cut sapphire substrate.

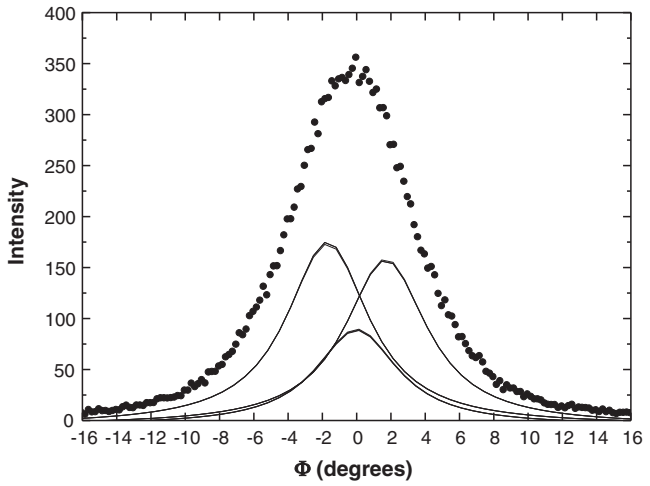

Fig. 5. φ scan on a pole recorded at $2\theta = 31.7°$ and $\psi = 50°$ for a gallium oxide film grown in a c-cut sapphire substrate at 500 °C under 10^{-5} mbar.

in Fig. 4b is related to the fact that in the $(\bar{2}01)$ (or (101)) plane of the β-Ga_2O_3 phase, the [132] and [102] directions (or $[\bar{1}31]$ and $[\bar{1}01]$ for the (101) plane) are separated by a 31.83° (or 31.74°) angle which is rather close to the 30° value which is the angle between the $[1\bar{1}0]$ and [100] of the sapphire substrate. Owing to the broad in plane extension of the poles presented in Fig. 3, it is not possible to distinguish between the two epitaxial relationships. Actually, precise φ scans were performed on various poles and a typical example is presented in Fig. 5. A broad peak with about 8° FWHM can be observed, and simulations were carried out to fit this curve. As shown in Fig. 5, it is possible to obtain a good fit by the sum of three peaks with a central one corresponding to the alignment described in Fig. 4b, and two other peaks located at ± 1.8° corresponding to the alignment of Fig. 4a. It can thus be concluded that the broad azimuthal extension of the poles can be due to the presence of the epitaxial relationships schematized in Fig. 4a and b.

Precise transmission electron microscopy and electron diffraction analyses have been recently carried out on $(\bar{2}01)$ oriented β-Ga_2O_3 films grown by Ga evaporation in oxygen plasma on c-cut sapphire substrates [37]. The results show that various in-plane orientations of the film on the substrate can exist, i.e., instead of a fixed 60° rotation between all the six variants, values of the rotation equal to 58.2 and 63.6° have been reported [37]. Such values are in agreement with the two distinct in-plane orientations described in Fig. 4b.

Table 2 shows that the lattice mismatch is almost the same for the epitaxial relationships of the two textures. Two questions have to be considered: (i) what is the origin of these particular $(\bar{2}01)$ and (101) textures, and (ii) why the $(\bar{2}01)$ texture is favored over the (101) one, the lattice mismatch being the same in the two cases.

First let us note that the (001) plane of the sapphire substrate is a polar plane with either solely oxygen or aluminum atoms. As a consequence, the first plane of the Ga oxide film would be preferentially a polar plane, either oxygen or gallium plane depending upon the nature of the surface plane of the sapphire substrate. The $(\bar{2}01)$ and (101) planes of the β-Ga_2O_3 phase being polar planes, the preferential growth of $(\bar{2}01)$ or (101) oriented crystallites would be thus favored with respect to the other non-polar planes of the β-Ga_2O_3 phase.

Then the precise atomic configuration in the $(\bar{2}01)$ and (101) planes of the β-Ga_2O_3 phase have to be taken into account to explain the fact that the $(\bar{2}01)$ plane is the most favorable for the epitaxial growth of the β-Ga_2O_3 phase on c-cut sapphire substrate. In this frame, considering as it is generally the case that the last atomic plane of the c-cut sapphire substrate is an oxygen plane, the first plane of the β-Ga_2O_3 film would be a Ga plane either $(\bar{2}01)$ or (101). Fig. 6 schematically represents the atomic configurations in these two planes, following

Table 2
Epitaxial relationships for Ga_2O_3 films on c-cut sapphire substrate for the (-201) and (101) textures. The corresponding matching and lattice matching are given.

Phase	Texture	Epitaxial relationships	Matching	Lattice mismatch
Monoclinic β	(−201)	$[102]_f$ // $[10.0]_s$	$1\ d_f \approx 3\ d_s$	$\delta \approx 2.8\%$
		$[010]_f$ // $[21.0]_s$	$8\ d_f \approx 3\ d_s$	$\delta \approx 1.7\%$
		$[132]_f$ // $[1\bar{1}.0]_s$	$1\ d_f \approx 2\ d_s$	$\delta \approx 4.8\%$
	(101)	$[\bar{1}01]_f$ // $[10.0]_s$	$1\ d_f \approx 3\ d_s$	$\delta \approx 3\%$
		$[010]_f$ // $[21.0]_s$	$8\ d_f \approx 3\ d_s$	$\delta \approx 1.7\%$
		$[131]_f$ // $[1\bar{1}.0]_s$	$1\ d_f \approx 2\ d_s$	$\delta \approx 4.8\%$

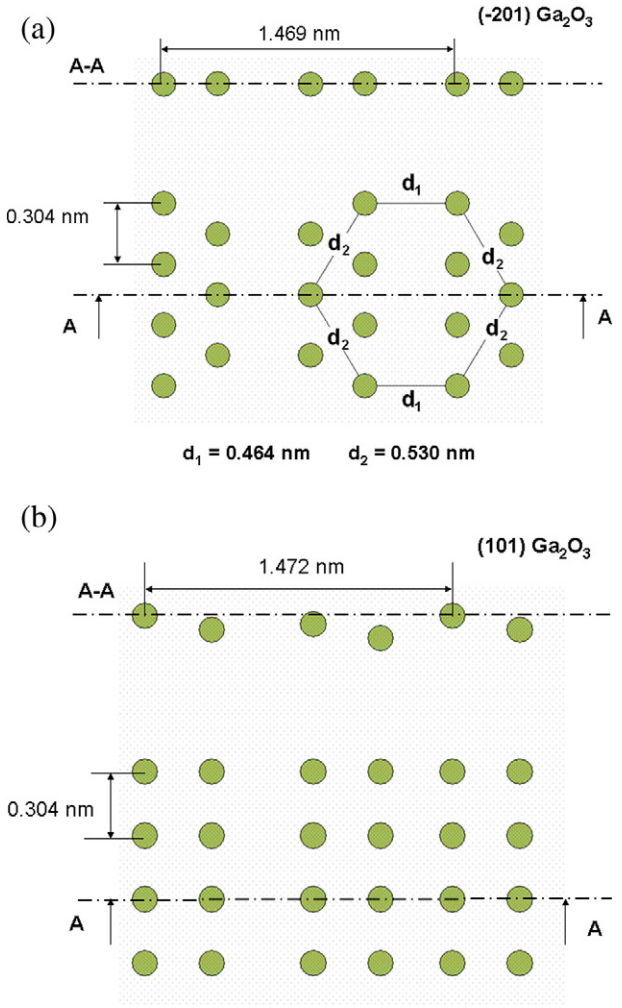

Fig. 6. Ga atoms' arrangement in the $(\bar{2}01)$ plane (a) and (101) plane (b) of the monoclinic β-Ga_2O_3 phase. The transverse sections show the positions of the atoms with respect to the plane.

the β-Ga_2O_3 crystal data reported [38]. In Fig. 6a corresponding to the $(\bar{2}01)$ β-Ga_2O_3 case, it must be noticed that all the Ga ions are perfectly located in the plane (see the transverse section A–A). Then these Ga ions are located in a configuration looking like an irregular hexagonal distribution. In fact the Ga–Ga ion distances are either 0.464 or 0.530 nm, leading to angles equal to 120.67 or 118.64° in the "hexagon like" configuration, instead of 120° in a regular hexagon.

On the other hand, in Fig. 6b corresponding to the (101) β-Ga_2O_3 plane, the Ga ions are not all located in such a plane as shown in the transverse section A–A. Moreover the Ga ions in the (101) β-Ga_2O_3 plane are aligned on parallel rows alternately separated by 0.667 or 0.807 nm. Such a Ga arrangement does not allow the formation of a hexagon like configuration similar to that present in the (0001) Al_2O_3 plane. In this case, the Ga ions of the (101) plane do not present a good coincidence with the oxygen from the substrate. From this Fig. 6a and b, the Ga atomic distribution in the $(\bar{2}01)$ plane seems more suitable to obtain a low interfacial energy due to the hexagon like configuration in this plane.

Another approach to understand the preferential $(\bar{2}01)$ texture with respect to the (101) one is to look at the oxygen sub-network. Actually in the oxide materials with a pronounced ionic character like Ga_2O_3, the crystalline structure depends mainly upon the oxygen sub-network. Indeed, owing to the difference in ionic radii, 0.14 nm and 0.083 nm for the oxygen and gallium ions respectively, the Ga cations behave like "interstitials" in the oxygen sub-network, ensuring the oxide stability through the Ga–O interactions. In such a case, the film epitaxy can be explained by considering the oxygen arrangement in the film as an almost continuous extension of the close packed anion network of the sapphire substrate [36,39]. In this frame, the epitaxial growth of the Ga oxide can be the result of the continuity of the oxygen sub-network through the film–substrate interface as it has been previously assumed [40]. For a long time it has been reported that $(\bar{2}01)$-oriented β-Ga_2O_3 thin film is formed on c-cut sapphire substrate owing to the similar oxygen arrangement of these planes [21,40]. However such a statement is not absolutely correct. Indeed, Fig. 7a represents the oxygen atoms distribution in this plane and as shown by the transverse section A–A, all the oxygen atoms are not really located in the plane. Then, considering only the oxygen atoms really in the plane, it can be noticed that these oxygen atoms present an irregular hexagon repartition with two O–O distances: 0.496 and 0.515 nm, while the oxygen distribution in the c-cut sapphire plane corresponds to a regular hexagon with a single one O–O distance equal to 0.476 nm.

For comparison purposes, Fig. 7b represents the oxygen atoms distribution in the (101) plane. First, the transverse section A–A that these atoms are not strictly located in the plane, and their distribution can correspond to three distinct irregular hexagons, whose dimensions are given in the table. By comparison with Fig. 7a, the schema (Fig. 7b)

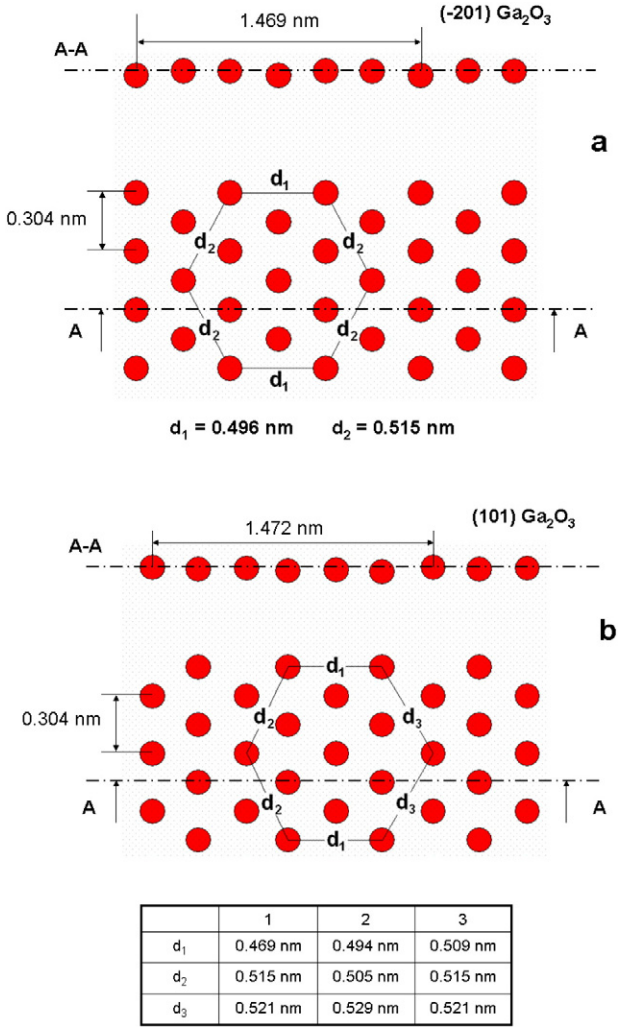

	1	2	3
d_1	0.469 nm	0.494 nm	0.509 nm
d_2	0.515 nm	0.505 nm	0.515 nm
d_3	0.521 nm	0.529 nm	0.521 nm

Fig. 7. Oxygen atoms' arrangement in the $(\bar{2}01)$ plane (a) and (101) plane (b) of the monoclinic β-Ga_2O_3 phase. The transverse sections show the positions of the atoms with respect to the plane.

shows a more important "disorder" in the oxygen atomic positions, leading thus to a large deformation of the hexagons of the oxygen sub-network in the (101) texture. This particular point could be at the origin of the preferential $(\bar{2}01)$ texture which is experimentally observed in this work.

4. Conclusion

The nature of the crystalline phase present in gallium oxide films grown by PLD on c-cut sapphire substrates has been studied. Under vacuum (10^{-7} mbar), polycrystalline films are obtained whose diffraction diagrams are compatible with the β or ε-Ga_2O_3 phases. At oxygen pressures higher than 10^{-5} mbar, amorphous gallium oxide films are formed, while in the intermediate range (10^{-7}–10^{-5} mbar), β-Ga_2O_3 epitaxial films are grown. Two distinct textures are observed with the $(\bar{2}01)$ and (101) planes parallel to the c-cut sapphire surface. The various epitaxial relationships were deduced from pole figure measurements, and the corresponding matching and lattice mismatch were obtained in the frame of the domain matching epitaxy. The $(\bar{2}01)$ texture seems to be more energetically favorable for the epitaxial growth owing to the atomic configuration of this plane.

References

[1] P. Wellenius, A. Suresh, J.F. Muth, Bright, low voltage europium doped gallium oxide thin film electroluminescent devices, Appl. Phys. Lett. 92 (2008) 021111–021113.
[2] T. Miyata, T. Nakatani, T. Minami, Gallium oxide as host material for multicolor emitting phosphors, J. Lumin. 87–89 (2000) 1183–1185.
[3] T. Harwig, F. Kellendonk, Some observations on photo-luminescence of doped β-gallium sesquioxide, J. Solid State Chem. 24 (1978) 255–263.
[4] Y. Kokubun, K. Miura, F. Endo, S. Nakagomi, Electrical characterization and hydrogen gas sensing properties of a n-ZnO/p-SiC Pt gate material semiconductor field effect transistor, Appl. Phys. Lett. 90 (2007) 031912–031913.
[5] M. Ogita, N. Saika, Y. Nakanishi, Y. Hatanaka, Ga_2O_3 thin films for high temperature sensors, Appl. Surf. Sci. 142 (1999) 188–191.
[6] M. Orita, H. Ohta, M. Hirano, H. Hosono, Deep-ultraviolet transparent conductive β-Ga_2O_3 thin films, Appl. Phys. Lett. 77 (2000) 4166–4168.
[7] E.G. Villora, K. Shimamura, K. Aoki, Rf-plasma-assisted molecular beam epitaxy of β-Ga_2O_3, Appl. Phys. Lett. 88 (2006) 031105-3.
[8] P. Marie, X. Portier, J. Cardin, Growth and characterization of gallium oxide thin films by radiofrequency magnetron sputtering, Phys. Status Solidi A 205 (2008) 1943–1946.
[9] S. Nakagomi, Y. Kokubun, Crystal orientation of β-Ga_2O_3 thin films formed on c-plane and α-plane sapphire substrates, J. Cryst. Growth 349 (2012) 12–18.
[10] V. Gottschalch, K. Mergenthaler, G. Wagner, J. Bauer, H. Paetzelt, S. Sturm, U. Teschner, Growth of β-Ga_2O_3 on Al_2O_3 and GaAs using metal–organic vapor-phase epitaxy, Phys. Status Solidi A 206 (2009) 243–249.
[11] A. Petitmangin, C. Hebert, J. Perrière, B. Gallas, L. Binet, P. Barboux, P. Vermaut, Metallic clusters in nonstoichiometric gallium oxide films, J. Appl. Phys. 109 (2011) 013711–013718.
[12] A. Petitmangin, PhD thesis, University Paris 6, Paris September 2010.
[13] K. Matsuzaki, H. Yanagi, T. Kamiya, H. Hiramatsu, K. Nomura, M. Hirano, H. Hosono, Field induced current modulation in epitaxial film of deep-ultraviolet transparent oxide semiconductor Ga_2O_3, Appl. Phys. Lett. 88 (2006) 092106-3.
[14] R. Huang, H. Hayashi, F. Oba, I. Tanaka, Microstructure of Mn-doped γ-Ga_2O_3 epitaxial films on sapphire (0001) with room temperature ferromagnetism, J. Appl. Phys. 101 (2007) 063526-6.
[15] S.S. Kumar, E.J. Rubio, M. Noor-A-Alam, G. Martinez, S. Manandhar, V. Shuttanandan, S. Thevuthasan, C.V. Ramana, Structure, morphology and optical properties of amorphous and nanocrystalline gallium oxide thin films, J. Phys. Chem. C 117 (2013) 4194–4200.
[16] L. Nagarajan, R.A. De Souza, D. Samuelis, I. Valov, A. Börger, J. Janek, K.D. Becker, P.C. Schmidt, M. Martin, A chemically driven insulator–metal transition in non-stoichiometric and amorphous gallium oxide, Nat. Mater. 7 (2008) 391–398.
[17] M. Nistor, A. Petitmangin, C. Hebert, W. Seiler, Nanocomposite oxide thin films grown by pulsed energy beam deposition, Appl. Surf. Sci. 257 (2011) 5337–5340.
[18] M. Nistor, J. Perrière, C. Hebert, W. Seiler, Nanocomposite indium tin oxide thin films: formation induced by a large oxygen deficiency and properties, J. Phys. Condens. Matter 22 (2010) 045006.
[19] J. Perrière, C. Hebert, A. Petitmangin, X. Portier, W. Seiler, M. Nistor, Formation of metallic clusters in oxygen deficient indium tin oxide films, J. Appl. Phys. 109 (2011) 123704–123708.
[20] E. Millon, M. Nistor, C. Hebert, Y. Davila, J. Perrière, Phase separation in nanocomposite indium tin oxide thin films grown at room temperature: on the role of oxygen deficiency, J. Mater. Chem. 22 (2012) 12179–12185.
[21] T. Oshima, T. Okuno, S. Fujita, Ga_2O_3 thin film growth on c-plane sapphire substrates by molecular beam epitaxy for deep-ultraviolet photodetectors, Jpn. J. Appl. Phys. 46 (2007) 7217–7220.
[22] P.P. Macri, S. Enzo, G. Sberveglieri, S. Groppelli, C. Perego, Unknown Ga_2O_3 structural phase and related characteristics as active layers for O_2 sensors, Appl. Surf. Sci. 65–66 (1993) 277–282.
[23] M. Orita, H. Hiramatsu, H. Ohta, M. Hirano, H. Hosono, Preparation of highly conductive, deep-ultraviolet transparent β-Ga_2O_3 thin film at low deposition temperatures, Thin Solid Films 411 (2002) 134–139.
[24] K. Matsuzaki, H. Hiramatsu, K. Nomura, H. Yanagi, T. Kamiya, M. Hirano, H. Hosono, Growth, structure and carrier transport properties of Ga_2O_3 epitaxial film examined for transparent field effect transistor, Thin Solid Films 496 (2006) 37–41.
[25] S. Yoshioka, H. Hayashi, A. Kuwabara, F. Oba, K. Matsunaga, I. Tanaka, Structure and energetics of Ga_2O_3 polymorphs, J. Phys. Condens. Matter 19 (2007) 346211-11.
[26] J. Narayan, K. Dovidenko, A.K. Sharma, S. Oktyabarsky, Defects and interfaces in epitaxial ZnO/α-Al_2O_3 and AlN/ZnO/α-Al_2O_3 heterostructures, J. Appl. Phys. 84 (1998) 2597–2601.
[27] P.R. Willmott, R. Timm, J.R. Huber, RHEED analysis of interface growth modes of TiN films on Si (001) produced by crossed beam laser ablation, Appl. Surf. Sci. 127–129 (1998) 105–110.
[28] C. Marechal, E. Lacaze, A. Laurent, J. Perrière, W. Seiler, Growth mechanisms of laser deposited BiSrCaCuO films on MgO substrates, Physica C 294 (1998) 23–32.
[29] W. Seiler, M. Nistor, C. Hebert, J. Perrière, Epitaxial undoped indium oxide thin films: structural and physical properties, Sol. Energy Mater. Sol. Cells 116 (2013) 34–42.
[30] N. Chaoui, E. Millon, J.F. Muller, P. Ecker, W. Bieck, H.N. Migeon, Perovskite lead titanate PLD films: study of oxygen incorporation by ^{18}O tracing techniques, Mater. Chem. Phys. 59 (1999) 114–119.
[31] J. Gonzalo, C.N. Afonso, J. Perrière, Influence of laser energy density on the plasma expansion dynamics and film stoichiometry during laser ablation of BISrCaCuO, J. Appl. Phys. 79 (1996) 8042–8046.
[32] E. Le Boulbar, E. Millon, J. Mathias, C. Boulmer-Leborgne, M. Nistor, F. Gherendi, N. Sbaï, J.B. Quoirin, Pure and Nd-doped $TiO_{1.5}$ films grown by pulsed-laser deposition for transparent p–n homojunctions, Appl. Surf. Sci. 257 (2011) 5380–5383.
[33] M.Y. Tsai, O. Bierwagen, M.E. White, J.S. Speck, β-Ga_2O_3 growth by plasma-assisted molecular beam epitaxy, J. Vac. Sci. Technol. A 28 (2010) 354–359.
[34] Y. Lv, J. Ma, W. Mi, C. Luan, Z. Zhu, H. Xiao, Characterization of β-Ga_2O_3 epitaxial films grown on MgO (111) substrates by metal–organic vapor deposition, Vacuum 86 (2012) 1850–1854.
[35] M. Nistor, F. Gherendi, N.B. Mandache, Angular distribution of species in pulsed energy beam deposition of oxide films, Appl. Surf. Sci. 258 (2012) 9274–9277.
[36] N. Sbai, J. Perrière, W. Seiler, E. Millon, Epitaxial growth of titanium oxide thin films on c-cut and α-cut sapphire substrates, Surf. Sci. 601 (2007) 5649–5658.
[37] S. Nakagomi, Y. Kokubun, Cross-sectional TEM imaging of β-Ga_2O_3 thin films formed on c-plane and α-plane sapphire substrates, Phys. Status Solidi A 210 (2013) 1738–1744.
[38] J. Ahman, G. Svensson, J. Albertsson, A reinvestigation of β-gallium oxide, Acta Cryst. C 52 (1996) 1336–1338.
[39] H.L.M. Chang, H. You, Y. Gao, J. Guo, C.M. Foster, R.P. Chiarello, T.J. Zhang, Structural properties of epitaxial TiO_2 films grown on sapphire (11–20) by MOCVD, J. Mater. Res. 7 (1992) 2495–2506.
[40] G.V. Chaplygin, A. Semiletov, Preparation, structure and electrical properties of epitaxial films of Ga_2O_3 on sapphire substrates, Thin Solid Films 32 (1976) 321–324.